Title

Using model identification to analyze spatially explicit data with habitat, and temporal, variability

Journal

Ecological Modelling, 214(2-4)

ISSN

0304-3800

Authors

Drury, Kevin L. S.
Candelaria, J. Fabian

Publication Date

2008-06-01

DOI

doi:10.1016/j.ecolmodel.2008.02.009

Peer reviewed

Using model identification to analyze spatially-explicit data with habitat, and temporal, variability

Kevin L. S. Drury †
†*National Center for Ecological Analysis and Synthesis (NCEAS)*
University of California, Santa Barbara,
Santa Barbara CA 93101
corresponding author: *drury@nceas.ucsb.edu*
and

J. Fabian Candelaria ‡
‡*Department of Mathematics,*
University of Puerto Rico, Arecibo Campus
candelaria.upra@gmail.com

Subject headings: Integrodifference equation, dispersal kernel, reaction-diffusion, spatially explicit model, model identification, model selection, California sea otter, Akaike Information Criterion, biological invasion, range expansion

Note: This is an author typeset verion of, Drury, KLS and JF Canderlaria. 2008. Using model identification to analyze spatially-explicit data with habitat, and temporal, variability. Ecological Modelling 214: 305–315.

Abstract

Range expansion rates vary by species, habitat, and time since initiation. These speeds are a key issue in the analysis of biological invasions and a wide variety of mathematical models address them. Many such models may provide an adequate estimate of invasion speeds, and hence, an adequate qualitative fit to spread data. In general, however, because of flexibility in choice of dispersal kernels, integrodifference equation (IDE) models are superior to reaction-diffusion (RD) models when spread rates increase through time. Nevertheless, additional differences in model complexity may arise through different approaches for dealing with habitat, and temporal, variability. This diversity of potential methodologies suggests the need for quantitative model selection criteria, although to our knowledge, IDE models have not been compared to RD models with diffusion that varies in space and time. To demonstrate our approach for choosing between a suite of spatially-explicit models that vary in complexity, we use the classic California sea otter range expansion data and the Akaike Information Criterion, which balances fit and parsimony. Our results show that the increasing speeds in the otter range expansion overwhelmingly support an IDE model for characterizing the entire data set. When focusing on certain stages of the range expansion, however, the more parsimonious reaction-diffusion model can provide the best description. Thus, the ideal spatial modeling framework can depend upon the temporal scale of the question.

1. Introduction

The rate at which invading organisms spread through new habitats is a key issue in the analysis of biological invasions. Since the seminal works of Fisher and Skellam (Fisher 1937; Skellam 1951) reaction-diffusion equations have been widely used to calculate these rates, which are often called invasion speeds, or "wave speeds". Thus, through long familiarity, the reaction–diffusion framework has become the workhorse of spatial ecology, where continuous space is concerned. Reaction-diffusion equations provide intuitive descriptions of interacting individuals that also redistribute themselves in space. Furthermore, when the interaction term is simple, these models can be solved analytically; most nonlinear forms, however, are intractable and must be solved numeri-

cally. Nevertheless, in the last $10-15$ years, with advances in desktop computing and mathematical ecology, integrodifference equation (IDE) models have proved similarly useful for analyzing spatio-temporal data (Kot et al. 1996). To our knowledge, however, these spatially-explicit modeling frameworks have not both been used to analyze the same data, and the results compared within a rigorous statistical framework. Thus, rather than rely on the popularity of reaction-diffusion models, we also used IDE models to analyze the classic data from the California sea otter (*Enhydra lutris*) range expansion, and let the data and the principle of parsimony dictate which has the most support through the Akaike Information Criterion (Burnham and Anderson 2002).

Although it is well-known that IDE models can generate accelerating invasion fronts (Kot et al. 1996), it is not obvious how they compare to reaction–diffusion models with diffusion that varies temporally. Casual inspection of the otter recolonization of the California coast (see e.g., Lubina and Levin 1988) suggests that spread rates do indeed vary, a characteristic shared with data from other invasions (Shigesada and Kawasaki 1997). Indeed, the otter data are rich in that spread rates appear to vary in both space and time, so that it is natural to ask, which modeling framework can best, and most parsimoniously, reproduce these patterns? In particular, is the increase in parameter number associated with treating habitats, and epochs, separately warranted? And, finally, do the answers to these questions change with the temporal scale of the question? To address these questions, we created a suite of RD and IDE models that vary in complexity and used standard model identification techniques (Burnham and Anderson 2002) to rank the models, using the sea otter data as arbiter. Because the otter data share features with data from other range expansions, our results are likely to be quite general.

2. Background and Natural History

The California sea otter is a keystone species (Estes et al. 1998) that was hunted to near extinction over most of its native range, including the coasts of much of the North Pacific ocean (Kenyon 1969). In 1914, however, a remnant population of otters was found at Point Sur, CA (Lubina and Levin 1988). Following protection, the otters have expanded their range with both northward and southward fronts along the coast. Range expansion occurs laterally along the coast because otters generally occupy a narrow band of coastline out to water depths ranging from 22m (Wendell 1994) to 40m (Laidre et al. 2001). Upon depletion of preferred prey within this band (Estes et al. 2003), otters switch to less favored prey (Ostfeld 1982), often altering community composition in the process (Kvitek et al. 1992), and eventually relocate to unexploited feeding areas (Garshelis and Garshelis 1984; Wendell et al. 1986; Wendell 1994).

Otter population density can drive resource depletion, and hence force range expansion, which occurs gradually (Garshelis et al. 1984) or by jumps of up to 127km for adults and 187km for subadults (Jameson 1989). Thus, the time-scale of range expansion is related, at least in part, to population increase. In California, otters usually have a single pup after 4–6 months gestation, followed by approximately 6 months post-natal dependency (Riedman et al. 1994). Otter births occur year-round, and although peak seasons have been noted (Garshelis et al. 1984), they have also been found insignificant (Riedman et al. 1994; Monson and DeGrange 1995). Accounts of survival are similarly variable (see e.g., Riedman et al. 1994; Monnett and Rotterman 2000), as are reported population growth rates. The maximum rate of increase is estimated at 20% per year, although 5–6% is more typical in California (Riedman et al. 1994).

3. Modeling Otter range expansion

Because otters reproduce year-round, but may show seasonal peaks, it is not clear whether models of continuous or discrete reproduction are most appropriate. Thus, to minimize the extent to which our results are driven by the time–scale of reproduction, we use the continuous logistic growth equation in our continuous-time RD models and its integral in our discrete-time IDE models. Differences between the predictions of the models should therefore primarily reflect differences in the way dispersal is modeled.

3.1. Population parameters

We estimated the instantaneous population growth rate $r = 0.056\text{yr}^{-1}$ of the logistic equation by calculating the best-fit straight line through log population size over the epoch for which it was approximately linear (Fig. 1a) (Lubina and Levin 1988). This estimate is similar to those obtained

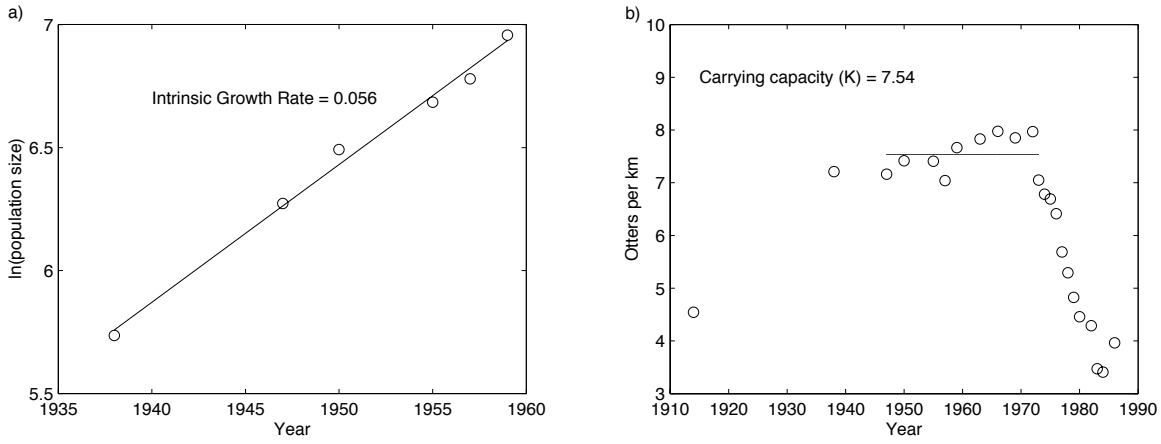

Fig. 1.— Estimates of population parameters for the California sea otter. a) The instantaneous population growth rate r. b) The carrying capacity K. See text for details of the estimation procedures.

by Riedman et al. (1994) ($r = 0.05$), Eberhardt (1995) ($r = 0.095$) and Eberhardt and Schneider (1994) ($r = 0.049$). To estimate carrying capacity $K = 7.54$/km, we averaged the population density during times for which the population density was relatively constant (Fig. 1b). Note that during these times, total population size and total range increased, but density taken over the entire population varied little. Other research corroborates the potential for sea otter habitat saturation in both California (Laidre et al. 2001) and Washington State (Laidre et al. 2002).

3.2. Reaction-diffusion and integrodifference equation models

To model reproduction and dispersal in continuous time, we used partial differential equation models, usually referred to as reaction-diffusion models in ecology (Murray 2002). Reaction-diffusion equations of the form,

$$\frac{\partial n(x,t)}{\partial t} = \overbrace{f(n(x,t))}^{reaction} + \overbrace{D\nabla^2 n(x,t)}^{diffusion}, \qquad (1)$$

have a long history in ecology (Holmes et al. 1994) and with the addition of advection (Lubina and Levin 1988) or diffusion coefficients that vary in space, can be used to model populations that spread at different rates in different directions. In Eq. (1) $n(x,t)$ is population density in space and time, $f(n)$ is a population growth function, D is the diffusion constant, t is time and ∇^2, known as the Laplacian, represents the second spatial derivative. In what follows, for readability, we suppress the subscripts (x,t), except where necessary for clarity.

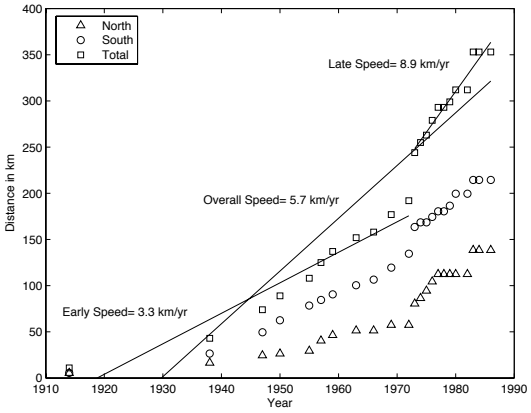

Fig. 2.— Range expansion of the California sea otter between 1914 and 1986 in the northward and southward directions, and total distance, from their source at Point Sur, CA. Note the relatively slow early expansion, followed by a relatively fast later phase.

As a model of spatial spread, Eq. (1) has several desirable features. For example, with relatively few parameters, it describes both local population dynamics and neighborhood diffusion. Nevertheless, some of the assumptions underlying Eq. (1) may make it inappropriate for analyzing some data. For example, continuous time implies

year-round reproduction, which is obviously only an approximation for seasonally reproducing animals. Additionally, the Laplacian implies that dispersal distances are normally distributed, which is unlikely to be universally applicable. Thus, in practice, using RD models requires these assumptions be satisfied, or alternatively, demonstrating that Eq. (1) balances parsimony with an adequate fit to the data better than more complex models that relax these assumptions.

Indeed, although the reaction-diffusion framework has proved useful in many applications (e.g., Fisher 1937; Skellam 1951), there are two relatively common features of range expansions that these models fail to capture. First, the beginning of many invasions are marked by relatively slow range expansion and then, following some threshold crossing (see, e.g., Mack et al. 2000), proceed at increased rates (Shigesada and Kawasaki 1997, chap. 2). This pattern (Fig. 2) is in contrast to the single, constant spread rate predicted by reaction-diffusion equations. Second, and closely related to such non-constant spread rates, many empirical distributions are leptokurtic, having thicker tails and narrower shoulders than the normal distribution (Kot 2003). Nevertheless, increasing the complexity of Eq. (1) so that diffusion $D(x,t)$ depends on both space and time could reasonably account for both these features of the data. Thus, although data from the entire range expansion may violate the assumptions of a simple version of Eq. (1), by comparing models of differing complexity, we can test the importance of such violations, relative to the importance of parsimony.

Additionally, because model identification procedures allow for comparison of models with differing numbers of parameters, we can simultaneously compare IDE models that also vary in complexity. IDE models sometimes provide more accurate predictions of invasion speeds, principally because of the wide variety of dispersal kernels they allow. For example, Kot et al. (1996) showed that the fat-tailed square root exponential dispersal kernel fit *Drosophila* dispersal data better than a suite of other forms. Such fat-tailed dispersal kernels generate increasing wave speeds in IDE models. We therefore compare a range of models in the reaction-diffusion partial differential equation family, that vary in detail from simple to complex, to integrodifference equations with a comparable range of complexity in dispersal kernels. This allows us to address the issue of temporal variability in range expansion rates with a single model description (IDE) or with diffusion that varies in time (RD). Similarly, we address the issue of spatial variability in spread rates by using separate dispersal kernels (IDE) and diffusion constants (RD) to analyze data from different habitats.

The basic integrodifference equation is,

$$n_{t+1}(x) = \int_{-\infty}^{+\infty} k(|x-y|) f(n_t(y))\, dy \qquad (2)$$

which is built around fundamentally different assumptions than reaction–diffusion. Eq. (2) relates the population size in the next time period, at any location x, to population growth at each spatial location y in the current time period and the probability of arriving at x from y. The first difference between this model and Eq. (1) is that time is discrete making this model appropriate for organisms that reproduce in pulses. For example, $n_t(x)$ is the population density at spatial location x in year t, while $n_{t+1}(x)$ is density at x the following year. Second, notice that $k(|x-y|)$, the dispersal kernel, can be any appropriate probability distribution and that the probability of moving from y to x depends only on the distance $|x-y|$. The population growth function, $f(n_t(y))$, is analogous to the reaction term in our reaction-diffusion equations.

The primary reason that Eq. (2) is an interesting and successful innovation in mathematical ecology is that different dispersal kernels make very different predictions about the rate of spread of organisms (Kot et al. 1996). Models with habitat or time-dependent dispersal kernels vary in parameter number, however, again suggesting the need for balance between model complexity and fit. Thus, quantitative methods for balancing the trade–off between flexibility and model complexity (i.e., parameter number) are especially important in pattern-rich data sets, such as the sea otter range expansion data.

3.2.1. Generalized exponential dispersal kernel for IDE models

In practice, we defined

$$z = |x-y|, \qquad (3)$$

so that $k(z)$ in Eq. (2) is the normalized kernel,

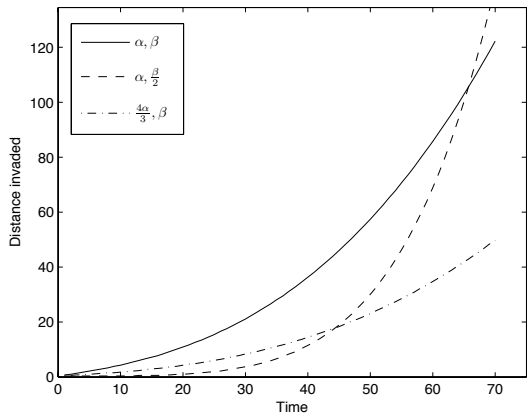

Fig. 3.— Effects of parameters of the generalized exponential kernel. Changes to α primarily affect the curvature of position vs. time, or the rate of change for the invasion wave. In contrast, changes to β primarily affect the position of the curve, thus affecting speed over the entire position vs. time curve.

$$k(z) = \frac{K(z)}{||K(z)||}, \tag{4}$$

where,

$$||f(x)|| = \int_{-\infty}^{+\infty} f(x)dx, \tag{5}$$

and,

$$K(z) = e^{-\alpha|z|^{\beta}}; \ \alpha, \beta \in \Re \geq 0. \tag{6}$$

Eq. (6) describes a simple symmetric kernel yielding identical dispersal in both directions. Note that if $\beta = 2$, Eq. (6) is the normal kernel used by the reaction diffusion model and that if $\beta < 1$, Eq. (6) becomes a generalization of the fat-tailed square root exponential kernel,

$$K(z) = e^{-\sqrt{z}}, \tag{7}$$

known to lead to accelerating wave fronts (Kot et al. 1996) such as those apparent in the otter data. Indeed, the maximum dispersal distances cited above in §2 suggest some form of fat-tailed dispersal kernel. Eq. (6) generalizes Eq. (7) in two ways. First, rather than specify the square root as the power (i.e., $\beta = 1/2$), we fit the spread rate to find the power β. Second, we multiply this root by a constant $\alpha > 0$, which rescales z. Note that Eq. (6) can generate a variety of spread rates, depending on α and β, but that whether the advantages of eq. (6) over eq. (7) outweigh the increase in parameter number is an empirical question that will be resolved by the $AICC$ calculation described in §4 − 4.1. Thus, by generalizing the square root exponential kernel described in Eq. (7), we allowed the data to specify the form of the kernel, rather than imposing an a priori shape.

Different choices of α and β in Eq. (6) modify the shape of the dispersal kernel and hence, alter the spread rate of the invasion. Indeed, the effects of α and β are most transparent when we consider their effects on population spread. Thus, to demonstrate the effects of α and β on population spread, we arbitrarily defined density $n = 0.01$ as the leading edge of the wave, numerically solved the model, and plotted invaded distance *vs.* time (Fig. 3). Decreases in β primarily alter the rate of change in the speed of the invasion wave. This can be seen in the population spread by an increase in the curvature of the distance *vs.* time curve (Fig. 3, dashed line). In contrast, increases in α primarily rotate the entire curve downwards, hence decreasing speeds, but have less effect on the rate of change in the speeds (Fig. 3, dash-dot line).

3.3. Numerical solutions

We used Forward-Euler methods with Neumann boundary conditions to numerically solve the reaction-diffusion equations. We used Matlab's implementation of the fast fourier transform, FFT, to convolve the integrals in the integrodifference equations. Finally, we used Matlab's $fminsearch$, an implementation of the Nelder-Meade simplex optimization algorithm (Press et al. 2002), to minimize the log-likelihoods. In both the RD and IDE modeling frameworks, we discarded initial model solutions and fit observed differences in the data to those predicted by the models after the solutions approached their long-time behavior. Our spatial discretization was $\Delta x = 0.01$, while in the RD framework, our temporal discretization was $\Delta t = 0.0001$. To increase flexibility, we multiplied the integer-valued observed range extent increases by the constant 1.815, which allowed for fractional predicted range increases, and hence smoother model predictions. Note that this transform affects α and β in the IDE results, but does not affect our estimates of c and D in the RD results. We calculated the constant speed of the advancing recoloniza-

tion front generated with the RD model by iterating the model until a constant speed c was approached, then solving the model for the duration of the epoch of interest and calculating $c = distance/time$. To calculate diffusion constants, we rearranged the well-known relationship,

$$c = 2\sqrt{rD}, \tag{8}$$

to obtain,

$$D = \frac{1}{r}\left(\frac{c}{2}\right)^2. \tag{9}$$

In the present case, speeds are in terms of $\frac{\text{km}}{\text{yr}}$ and diffusion constants in terms of $\frac{\text{km}^2}{\text{yr}}$. Our initial population distribution was $\tilde{x}$, the 11km remnant population at Point Sur, CA (Lubina and Levin 1988).

4. The likelihood function and model identification

Given data and a suite of models, model identification procedures use a likelihood function to quantify the fit of each model to the data. Such likelihood functions specify the stochastic distribution of observations around the deterministic expectation (i.e., the model prediction). Note that because the cumulative otter range extents are not independent in time, we do not fit our models to the cumulative range expansion. Instead, we assume that the differences in range extent from year-to-year are normally distributed around the predicted differences of the deterministic model. Specifically, letting L_j be the likelihood of the j^{th} transition in the data d_j (i.e., the range increase between times t and $t+1$), given model transition m_j, the assumption of normality yields,

$$L_j = (m_j - d_j)^2. \tag{10}$$

Thus, the likelihood L of all the range increases is the sum of the squared errors between each predicted model range increase, and the observed range increases in the data. Note that this approach assumes measurement-error-only, which we deem acceptable given the resolution of the data, but that process error can also be incorporated in such analyses (see e.g., Wikle 2003; Hooten et al. 2007).

4.1. Δ_i and strength of evidence

To avoid over-fitting, a model identification procedure must penalize more complex models for additional parameters. Thus, we used the corrected Akaike Information Criterion ($AICC$), which provides a quantitative means of identifying models that are both most parsimonious and best supported by the data (Burnham and Anderson 2002). The AIC is a likelihood-based statistic that allows comparison of multiple hypotheses or models (Taper 2004). Specifically, letting $L_i(\hat{\theta}_i)$ be the likelihood of model i with maximum-likelihood parameter(s) $\hat{\theta}_i$, number of model parameters k_i, and number of observations n_i, $AICC_i$ is given by,

$$AICC_i = \overbrace{-2log(L_i(\hat{\theta}_i)) + 2k_i}^{\text{AIC}} + \overbrace{\frac{2k_i(k_i+1)}{n_i - k_i - 1}}^{\text{small sample correction}}. \tag{11}$$

In practice, letting AIC^* be the lowest $AICC_i$ score, we calculated Δ_i as the difference between the $AICC_i$ of the i^{th} model and AIC^*. That is

$$\Delta_i = AICC_i - AIC^*. \tag{12}$$

Models generating $AICC_i$ such that $\Delta_i \geq 2$ are statistically distinguishable from the model generating AIC^*, while $\Delta_i \geq 5$ indicates very strong support for the best model, making Δ_i a useful metric for interpreting results (Taper and Gogan 2002). Note that such inferences depend on both the suite of models considered, and the data. In other words, if additional data were available, the model yielding AIC^* could change. Similarly, if additional information became available that suggested a new model, the rank order of Δ_i could change. Far from being a weakness, this is a strength of the approach because, given current information, it ensures we use the model(s) with the lowest estimate(s) of the expected, relative distance between the model(s) and the generally unknowable true mechanism that generated the observations (Burnham and Anderson 2002).

5. Model variants suggested by the data

5.1. Case 1: Singe dispersal kernel

Fitting a single model to all the data suggests that habitat-, and time-specific differences

in spread are not important. Thus, this approach reveals the most general description of the data, and treats any spatial and temporal variability as noise around the deterministic prediction of a single reaction-diffusion process. The simplest RD model we considered for this purpose was Eq. (1) with, $f(n)$ represented by logistic growth,

$$f(n) = rn(1 - \frac{n}{K}), \tag{13}$$

where here and in all the following models r is the intrinsic population growth rate and K is the carrying capacity. In Eq. (1), D is the diffusion constant, which in this case is the same in both directions (the shoreline can usefully be thought of as one-dimensional). Eq. 1 serves as our null hypothesis because more detailed models must overcome penalties for the additional parameters accompanying increased model complexity. For example, movement rates may be importantly different in the northward and southward directions, or more generally, in different habitats. As discussed above, this trend is indeed qualitatively apparent in the sea otter range expansion data (Fig. 2a), though its relative importance remains unquantified.

Similarly, the simplest integrodifference equation we analyzed has a single, symmetric dispersal kernel. Removing the absolute value from eq. (2) to address asymmetric kernels later, gives us the general integrodifference equation

$$n_{t+1}(x) = \int_{-\infty}^{+\infty} k(x-y) f(n_t(y)) dy, \tag{14}$$

where

$$f(n_t(x)) = \frac{Ce^{rt}}{(1 + \frac{C}{K}e^{rt})}, \tag{15}$$

is the integral of the logistic growth equation with initial population size C.

5.2. Case 2: Separate north and south dispersal kernels

Northward and southward spread rates may be different because of habitat differences along the California coast, which alter the rate that otters colonize new territories. Although the otter spread rate data suggest that northward range expansion was slower than southward, it is not at all obvious whether this difference warrants additional model parameters or whether a single diffusion constant can adequately describe both rates, by essentially averaging them. To test whether separate northward and southward diffusion constants are warranted, we allowed the diffusion coefficient to vary in space $D(x)$,

$$\frac{\partial n}{\partial t} = f(n) + D(x)\nabla^2 n, \tag{16}$$

with $D(x)$ given by,

$$D(x) = \begin{cases} D_n, & x > \tilde{x} \\ D_s, & x \leq \tilde{x}. \end{cases} \tag{17}$$

Here D_n represents the northward diffusion constant, D_s the southward diffusion constant, and $\tilde{x}$ the location of the remnant source population.

Another way to account for the southward bias in the data is to include an advection term in the reaction-diffusion equation as Lubina and Levin (1988) did, giving,

$$\frac{\partial n}{\partial t} = f(n) + D\nabla^2 n + a\frac{\partial n}{\partial x}. \tag{18}$$

Equation (18) says that the population changes according to $f(n)$, diffusive spread, and advective displacement, which shifts the center of the distribution at a rate, and direction, governed by the magnitude and sign, respectively, of a. Thus, Eq. (18) suggests that diffusion rates are identical in northerly and southerly habitats, but that southerly coastal currents hinder net northward spread and accelerate net southward spread. While advection provides a plausible hypothesis for the southward bias in spread rates, after careful analysis of the otter data and the conditions on the California coast, Lubina and Levin (1988) conclude that advection is unlikely to account for the bias in this case, and so we do not consider it further here.

To accommodate differences in the speed of range expansion in the northward and southward directions for the IDE model, we created an asymmetric version of the exponential dispersal kernel. In this case, with z given by Eq. (3), $k(z)$ can be defined by cases analogous to eq. (17). Specifically,

$$k(z) = \begin{cases} k_s = \exp(-\alpha_s z^{\beta_s}), & x < \tilde{x}, \\ k_n = \exp(-\alpha_n z^{\beta_n}), & x \geq \tilde{x}, \end{cases} \tag{19}$$

where $\tilde{x}$ is again Point Sur, CA, the boundary between the northward and southward fronts. The kernel in Eq. (19) thus allows for distinct dispersal probability distributions for the northern and southern habitats, although with twice the number of parameters of Eq. (17).

5.3. Case 3: Separate early and late dispersal kernels

Inspection of both the northward and southward sea otter range expansion data reveals an obvious discontinuity in spread between $\tilde{t} = 1972$ and 1973. Furthermore, the rates of spread before and after this event appear to be substantially different, with range expansion proceeding at much faster rates post-1972. These features of the data suggest a temporal partition into pre–1973 and post–1973 epochs, which we call the early e and late l epochs.

Allowing diffusion rates $D(t)$ to vary with time yields,

$$\frac{\partial n}{\partial t} = f(n) + D(t)\nabla^2 n, \tag{20}$$

where

$$D(t) = \begin{cases} D_e, & t < \tilde{t}, \\ D_l, & t \geq \tilde{t}. \end{cases} \tag{21}$$

A similar temporal partition in our IDE model yields two equations, one for the early epoch and one for the late, with the difference appearing in the parameters of the dispersal kernel,

$$k(z) = \begin{cases} k_e = \exp(-\alpha_e z^{\beta_e}), & t < \tilde{t}, \\ k_l = \exp(-\alpha_l z^{\beta_l}), & t \geq \tilde{t}. \end{cases} \tag{22}$$

5.4. Case 4: Different early, late, north, and south rates

Cases 2 and 3 allow us to evaluate the relative importances of habitat differences and temporal differences in sea otter spread rates. Despite the potential for superiority of one of these, models that account for both may also be useful. Thus, because of the apparent increase in rate with time in both directions, we also explored a model with an early and late diffusion coefficient for both the north and south directions. This resulted in four values of $D(x,t)$,

$$\frac{\partial n}{\partial t} = f(n) + D(x,t)\nabla^2 n, \tag{23}$$

where

$$D(x,t) = \begin{cases} D_{n,e}, & x > \tilde{x} \text{ and } t < \tilde{t}, \\ D_{n,l}, & x > \tilde{x} \text{ and } t \geq \tilde{t}, \\ D_{s,e}, & x \leq \tilde{x} \text{ and } t < \tilde{t}, \\ D_{s,l}, & x \leq \tilde{x} \text{ and } t \geq \tilde{t}. \end{cases} \tag{24}$$

Thus, diffusion proceeds at the slow (or fast) northward (or southward) rate, depending whether the range expansion is in the early (or late) stages, and whether the spread occurs north (or south) of $\tilde{x}$. Note that this approach remains valid in the more general case in which temporal discontinuities do not occur simultaneously in the habitats (i.e., $\tilde{t}_i$, $i \in (n,s)$ could represent distinct discontinuities in the northward and southward data). The analogous cases for spatial and temporal division of the IDE dispersal kernels yield,

$$k(z,t) = \begin{cases} k_{n,e} = \exp(-\alpha_{n,e} z^{\beta_{n,e}}), x > \tilde{x} \text{ and } t < \tilde{t}, \\ k_{n,l} = \exp(-\alpha_{n,l} z^{\beta_{n,l}}), x > \tilde{x} \text{ and } t \geq \tilde{t}, \\ k_{s,e} = \exp(-\alpha_{s,e} z^{\beta_{s,e}}), x \leq \tilde{x} \text{ and } t < \tilde{t}, \\ k_{s,l} = \exp(-\alpha_{s,l} z^{\beta_{s,l}}), x \leq \tilde{x} \text{ and } t \geq \tilde{t}. \end{cases} \tag{25}$$

6. Results

Because of the obvious increase in spread rates over time (Fig. 4a-b, dashed lines), an IDE model captures the character of the data substantially better than reaction-diffusion (i.e., Case 1, §5.1, Tab. 1, rows 1 and 2). Note that because we fit observed range expansion differences, the best-fit models do not divide the northward and southward fronts equally, as they would had we fit cumulative distance. Analysis of residuals reveals that the uncharacteristically large differences, in both directions, at 1972 cannot be accommodated by either modeling framework. In other words, the extreme difference that candidate models must generate to fit the 1972-1973 transition adequately generates poor fits to all other transitions. Thus, although the best-fit combined IDE divides the northern and southern fronts nicely up to 1972 (Fig. 4b), the modest model transition to 1973 results in the remaining model prediction lying well

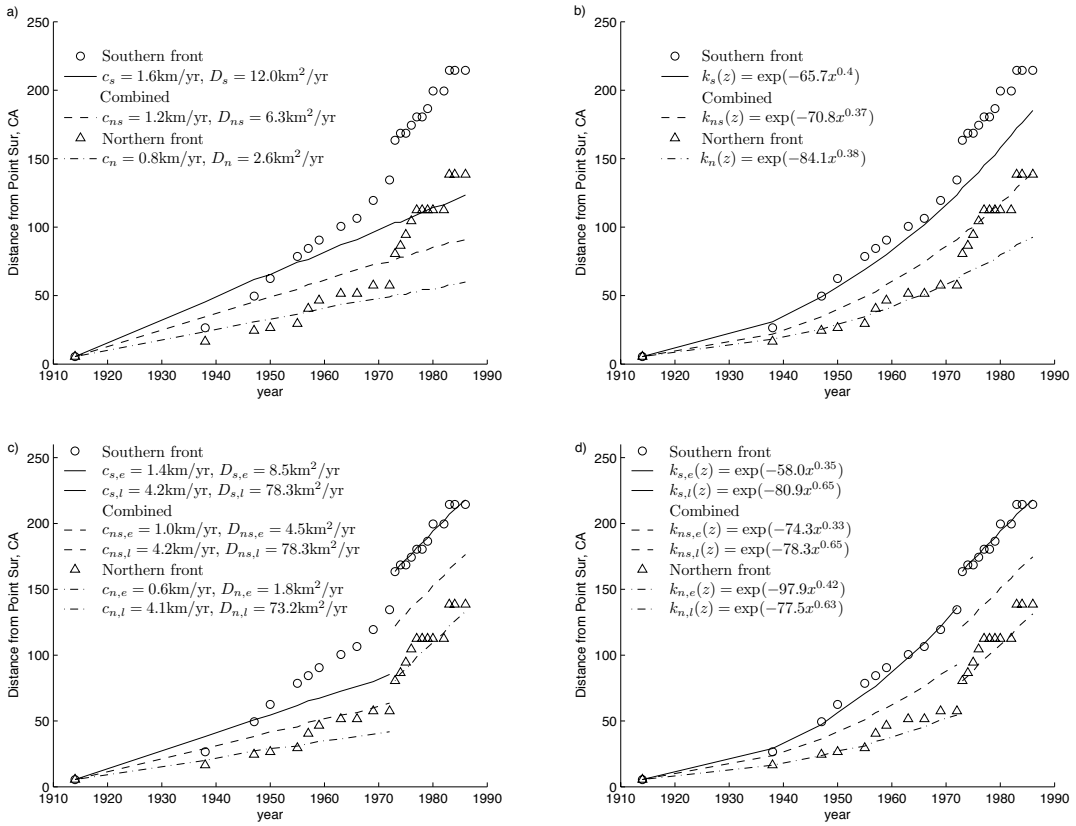

Fig. 4.— a) Best reaction-diffusion models when northward and southward data are treated as coming from habitats with distinct parameters, as well as the best single model that treats the northward and southward fronts as arising from different realizations of the same diffusion process. The wave speeds c_i and diffusion constants D_i are calculated using the entire data set spanning 1914-1986. b) As in (a) except that the best northward, southward, and single integrodifference equations are superimposed over the data. The $k_i(z)$ are parameterized generalizations of the square-root exponential dispersal kernel. c) Best northward, southward, and combined reaction-diffusion models for the early e (1914-1972) and late l (1973-1986) epochs. d) As in (c), except the models are integrodifference equations with parameterized dispersal kernels $k_i(z)$.

below the average of the two fronts. Note, however, that the curvature of the IDE model after 1973 is similar to that of both the northward and southward fronts for this epoch.

Separating the data into separate northward and southward components (i.e., Case 2, §5.2) yields similar results, with the IDE models again providing a substantially better fit (Fig. 4a-b, solid and dash-dot lines). Additionally, note that although the number of parameters doubles with this habitat-based division of the data, the Δ_i values are far smaller than the corresponding single-model results, indicating that the increase in parameter number provides a meaningful improvement (Tab. 1, rows 3 and 4), with the corresponding inference that otter dispersal rates vary importantly by habitat.

Even after allowing for habitat differences, both the RD and IDE model again fail to account for the 1972 transition. Additionally, obvious differences exist between early (pre-1973) and late (post-1973) spread rates, a feature the otter range expansion shares with other invasions (i.e., Case 3, § 5.3). To address the importance of these temporal differences, we again fit both the reaction-diffusion and IDE models simultaneously to the northward and southward data, but in two separate epochs (Fig. 4c-d, dashed lines). This separation reduces the number of observations we are fitting as well, however, because the abnormally large transition between 1972 and 1973 is no longer included. Thus, these Δ_i values are not directly

Table 1: Results of model identification using all the data (rows 1-4), and a division of the data into an early (1914-1972) and late epoch (1973-1986) (rows 5-8) and using Δ_i from Eq. (12) as the model identification criterion.

Modeling Framework	**Separate directions?**	**Separate epochs?**	**Eq.**	**Fig.**	**k**	**n**	L	Δ_i
Reaction-Diffusion	no	no	1,13	4a	1	44	3499.1	1227.6
Integro-difference	no	no	14,15	4b	2	44	2591.7	322.4
Reaction-Diffusion	yes	no	16,17	4a	2	44	3319.6	1050.3
Integro-difference	yes	no	19	4b	4	44	2264.6	0
Reaction-Diffusion	no	yes	20,21	4c	2	42	1959.8	796.7
Integro-difference	no	yes	22	4d	4	42	1561.2	402.9
Reaction-Diffusion	yes	yes	23,24	4c	4	42	1737.7	579.4
Integro-difference	yes	yes	25	4d	8	42	1147	0

NOTE.—k is the number of model parameters, n is the number of transitions in the data used in the comparison. Δ_i values ≥ 5 indicate very strong evidence against a model, and thus provide strong support for the model that generates $\Delta^* = \min_i\{AICC_i\}$.

comparable to those obtained from the full data set, because differences arise from the combination of discarding the problematic 1972 transition, and any differences in the ability of the model to account for the remaining transitions. Also note that in (Fig. 4c-d), both model predictions for the late epoch are pictured as beginning at the average between the northward and southward 1973 fronts. This provides a convenient, though somewhat arbitrary, means of comparing the model to both fronts, but recall that the models were fit to the transitions, not the cumulative ranges.

With temporal division of the data, the IDE again provides the better fit of the two modeling frameworks (Tab. 1, rows 5 and 6). Nevertheless, because habitat division did provide an improvement over treating the entire data set as a whole, we divided the data further into both northward and southward components, and early and late epochs (i.e., Case 4, §5.4, Fig. 5a-b). This comparison reveals that despite the relatively large number of parameters (i.e., 8), the IDE model is overwhelmingly supported by the data (i.e., Tab. 1, rows 7 and 8), indicated by $\Delta_i = 0$ for the IDE model and all other $\Delta_i \gg 5$.

Although the IDE overwhelmingly fit these particular divisions of the data best when considering the entire time span from 1914-1986, the difference in likelihoods between the reaction-diffusion and IDE models for the late epoch from 1973-1986 was trivial. This lack of difference, expected in spread rate data that are essentially constant through time, motivated us to explore comparisons between RD and IDE models within particular epochs. If the initial transition 1914-1938 (T1) is also treated separately, data from the intermediate epoch 1938-1973 (T2) appear approximately linear, from both the northward and southward fronts, suggesting 3 piece-wise linear range expansion epochs. Because the initial epoch (i.e., 1914-1938) contains only two observations, it can be matched perfectly by both modeling frameworks and contributes nothing to the likelihoods. Differentiating between the two frameworks in such cases is a trivial matter of comparing parameter numbers. We nevertheless show the best fit reaction-diffusion model during T1 in order to present the northward and southward speeds and diffusion constants (Fig. 5a) of this initial phase of the recolonization process.

Such divisions of the data into discrete epochs cannot continue indefinitely if we are to make meaningful generalizations about spread rates. Nevertheless, the approximate linearity of the data in the middle (T2) and late (T3) epochs is suggestive, and reinforces the need for quantitative methods of distinguishing between the modeling frameworks (Fig. 5a-b). When both the middle and late epochs are considered, the IDE model again receives the most support from the data (i.e., Tab. 2, rows 1 and 2). In contrast, when only the late epoch (T3) is considered, the additional parameters of the IDE model generate

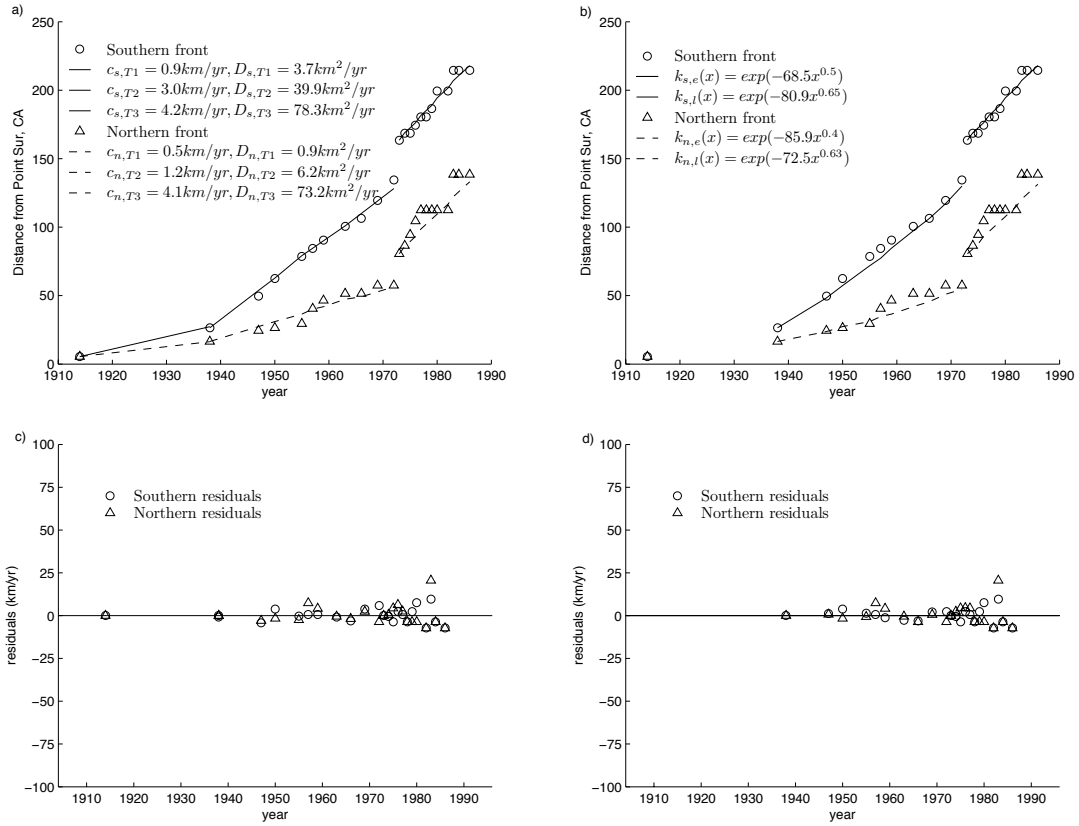

Fig. 5.— a) Best reaction-diffusion models when spread is separated into three epochs, an initial establishment phase 1914-1938 ($T1$), an initial spread phase 1939-1972 ($T2$), and a late spread phase 1973-1986 ($T3$). Because epoch $T1$ only contains one interval, both reaction-diffusion and integrodifference equations can match it perfectly. We nevertheless show the best fit reaction-diffusion model to quantify speed and diffusion during this epoch. b) As in (a) using integrodifference equations with separate dispersal kernels for each direction and epoch. c) Differences between observed and predicted southward and northward range increases per time interval for the reaction-diffusion models of panel (a). d) Differences between predicted and observed southward and northward range increases per time interval for integrodifference equation models of panel (b).

a modestly larger Δ_i than the reaction-diffusion model, despite a lower likelihood (i.e., Tab. 2, rows 3 and 4). Thus, RD provides the best and most parsimonious description of the data over the 13 years of T3.

7. Discussion

Our results show that standard model selection techniques can be useful for quantitatively choosing between a suite of spatial models, each providing reasonable approximations to spread data from a biological invasion. This is significant, because both reaction-diffusion models (Lubina and Levin 1988), and IDE models (Krkošek et al. 2007), have been successfully used to model numerous invasions, including the sea otter range expansion. Indeed, the otter data shares features with a growing number of range expansion data sets (Shigesada and Kawasaki 1997) that render the best modeling framework far from obvious. For example, are spread rates that vary in time best addressed with piecewise constant spread associated with temporally variable diffusion, or with IDE models that predict accelerating wave speeds? Without rigorous model identification procedures, it is not clear how to balance the need for adequate representation of such patterns in data with the additional parameters of more complex models. Such ambiguity is perhaps most apparent when detailed in-

Epoch	Modeling Framework	Eq.	Fig.	k	n	L	Δ_i
1938-1972 & post-1973	Reaction-Diffusion	23,24	5a	4	40	1158.0	46.4
	Integro-difference	25	5b	8	40	1100.1	0
post-1973 only	Reaction-Diffusion	23,24	5a	2	22	952.2	0
	Integro-difference	25	5b	4	22	950.3	3.9

Table 2: Results of model identification using the middle epoch (1938-1972) with the late epoch (1973-1986) (rows 1-2), as well as the late epoch alone (rows 3-4). We used Δ_i from Eq. (12) as the selection criterion, k is the number of model parameters and n is the number of data transitions used to fit the model. $2 < \Delta_i \leq 5$ indicate strong, but not very strong, evidence against a model.

formation about movement behavior of individuals is not available. In such cases, approaches such as ours could be used to provide initial estimates of the probability distribution of individual dispersal distances, through inference from population-level observations.

Our quantitative analysis shows that more complex models may address large-scale patterns in range expansion data better than simple models. This result depends on the temporal scale of analysis, however. For example, when fitting data over the entire otter recolonization epoch, more complex models fit the data substantially better. In particular, the accelerating wave speed associated with fat-tailed exponential dispersal kernels in the integrodifference equation framework fits the curvature in the range expansion data exceptionally well. This would presumably also be true for other data with increasing spread rates. In contrast, when analyzing spread rates within a particular habitat, over epochs of shorter duration, the constant spread rate generated by reaction-diffusion models generated lower $AICC$ scores. This arose despite the IDE having a lower likelihood for the data in question, because penalties for additional parameters increase the IDE $AICC$ score above that of the reaction-diffusion model. Again, this is likely to be a general feature of approximately linear subsets of range expansion data.

Treating the northern and southern fronts as arising from separate habitats provides a large improvement over treating them as different realizations of the same dispersal process. This suggests that ignoring these differences and estimating spread rates with a composite of the northward and southward fronts would miss important habitat-based differences in sea otter dispersal. Indeed, sea otter ecology corroborates the potential for habitat differences to drive the difference between northward and southward spread rates. For example, south of the point of origin at Point Sur, rocky intertidal gives way to less preferred sandy-bottomed shore line. Because otter dynamics are sensitive to pup survival (Monnett and Rotterman 2000), the lack of sheltered coves in sandy central California, as well as rapid changes in the soft-bottomed invertebrate communities post-otter arrival (Wendell et al. 1986), may lead to more rapid traversal through the southern range. Such expansions typically occur when aggregations of males leave areas with depleted food resources, and move into adjacent, previously unoccupied areas. Thus, they presumably continued southward to find unexploited resources rather than turn northward and move back into occupied territory. Females then typically expand into areas previously occupied by males (Garshelis et al. 1984). Apparently, the suitable habitat along the rockier coast of northern California leads to less rapid exploration of new areas.

Within both the habitat-independent and habitat-dependent results, the IDE had a substantially lower $AICC$ score than the RD, suggesting that flexibility in the dispersal kernel is of paramount importance for matching the otter re-expansion data. Indeed, although the range expansion occurred at different rates in the northward and southward directions, it accelerated in both directions, a feature not possible when dispersal occurs via diffusive spread. Furthermore, temporal differences in the rates of advance of the northward and southward fronts may be more important than habitat differences, because the results of analyses in which we ignored habitat differences and temporally divided the data into early and late epochs, generated lower $AICC$ scores than those generated by differentiating based on habitat alone. We cannot make strong inferences

about this result, however, because discarding the 1972-73 transition creates a new data set and information theoretic techniques cannot be used to compare fits to different data sets. Nevertheless, employing both habitat and temporal divisions (i.e., the reduced data set) provided the best fit, with the IDE model receiving the lowest $AICC$ of all.

The realities of otter range expansion are nevertheless far more complex than any of the models we explored. For example, exploration of new territories by sea otters is often carried out disproportionately by adult males (Garshelis et al. 1984). None of our models is age-, stage-, or size-structured, making all our descriptions of the processes phenomenological approximations (for a treatment with stage-structure, see Krkošek et al. 2007). Furthermore, the ecological description in §2 suggests density-dependent dispersal. Nevertheless, when faced with growing numbers of invading organisms, or the potential for large-scale shifts in species ranges, generalized models that can adequately describe existing data provide useful first approximations to future spread. In this context, it is useful to compare some conclusions from our results to those of previous investigators. The spread rates we calculated from our RD model compare quite favorably with those Lubina and Levin (1988) calculated using linear regression. For example, Lubina and Levin (1988) report the southern spread rate as 3.1km/yr between 1938 and 1972, while our model predicts it as 3.0km/yr for the same habitat and time span. Similarly, Lubina and Levin (1988) report the northern spread rate for the same time interval as 1.4km/yr while our model predicts 1.2km/yr. The agreement between our model and their regressions is similarly good for other habitat, and time, partitions.

Lubina and Levin (1988) also provide estimates of the diffusion constant D, derived by regressing mean-square-distance on time (Kareiva 1983), which can be compared to the estimates generated by our model. Though calculated with a different technique and for different epochs, the results are nevertheless consistent, so that our estimates complement theirs to provide additional information about otter dispersal. Note that this information relates to RD models only, but as we have shown, these models sometimes provide the best description of sea otter range expansion. For the years 1968–1974, Lubina and Levin (1988) report diffusion rates in the north of $D = 13.5\text{km}^2/\text{yr}$ and in the south, $D = 54.7\text{km}^2/\text{yr}$. Because of differences in methodology, we did not estimate diffusion rates for this particular interval, but our results bracket these in terms of time interval and, encouragingly, in terms of diffusion rates. Specifically, for the middle epoch (T2) 1938–1972, we calculated northward diffusion as $D_{n,T2} = 6.2\text{km}^2/\text{yr}$ and southward diffusion as $D_{s,T2} = 39.9\text{km}^2/\text{yr}$. Both these values are less than those reported for 1968–1974, which is to be expected, because that time interval contains the abnormally large range jumps that occurred between 1972–1973. Similarly, our late epoch (T3) estimates exclude slower movement rates prior to 1972 included by Lubina and Levin (1988). Our estimates from 1973-1986, $D_{n,T3} = 73.2\text{km}^2/\text{yr}$ and $D_{s,T3} = 78.3\text{km}^2/\text{yr}$ therefore exceed those reported by Lubina and Levin (1988). Thus, to the extent that diffusion adequately describes sea otter population spread, our estimates of diffusion both before and after the 1972 anomaly are consistent with previously published rates, and may be useful for forecasting future otter range expansions in similar habitats.

Populations obviously cannot continue to expand their range at increasing rates, or even constant rates, indefinitely. Nevertheless models with these characteristics may provide the best predictions over realistic time horizons. Indeed, IDE models with generalizations of the square root exponential dispersal kernel capture the character of the sea otter range expansion exceedingly well. When spread rates from particular habitats and epochs are of interest, however, the simpler RD model sometimes proves most useful, through the combination of adequate fit and parsimony.

Acknowledgments

This work began as a project at a National Science Foundation funded VIGRE mini-course in the Mathematics Department at the University of Utah. The authors therefore thank the organizers, Fred Adler, Mark Lewis, and Mike Neubert. KLSD also wishes to gratefully acknowledge support from a GAANN training grant to the Department of Ecology and Evolution at The University of Chicago, support from David Lodge at the Department of Biological Sciences, University of Notre Dame, and support from the Mellon Foundation to Mark Schildhauer and Matt Jones of NCEAS, and Judith Kruger of Kruger National Park, South Africa. The authors are grateful for comments from 3 anonymous reviewers, which

greatly improved the clarity of the manuscript.

REFERENCES

Burnham, K. P. and D. R. Anderson. 2002. Model selection and multimodel inference: A practical information-theoretic approach. Springer-Verlag, New York.

Eberhardt, L. L. 1995. Using the lotka-leslie model for sea otters. Journal of Wildlife Management **59**:222–227.

Eberhardt, L. L. and K. B. Schneider. 1994. Estimating sea otter reproductive rates. Marine Mammal Science **10**:31–37.

Estes, J. A., M. L. Riedman, M. M. Staedler, and M. T. Tinker. 2003. Individual variation in prey selection by sea otters: patterns, causes and implications. J. Anim. Ecol. **72**:144–155.

Estes, J. A., M. T. Tinker, T. M. Williams, and D. F. Doak. 1998. Otters linking oceanic and nearshore ecosystems. Science **282**:473–476.

Fisher, R. A. 1937. The wave of advance of advantageous genes. Annals of Eugenics **7**:255–369.

Garshelis, D. L. and J. A. Garshelis. 1984. Movements and management of sea otters in alaska. Journal of Wildlife Management **48**:665–678.

Garshelis, D. L., A. M. Johnson, and J. A. Garshelis. 1984. Social organization of sea otters in prince william sound, alaska. Can. J. Zool. **62**:2648–2658.

Holmes, E. E., M. A. Lewis, J. E. Banks, and R. R. Veit. 1994. Partial-differential equations in ecology - spatial interactions and population-dynamics. Ecology **75**:17–29.

Hooten, M., C. Wikle, R. Dorazio, and J. Royle. 2007. Hierarchical spatiotemporal matrix models for characterizing invasions. Biometrics **63**:558–567.

Jameson, R. J. 1989. Movements, home range, and territories of male sea otters off central califonia. Marine Mammal Science **5**:159–172.

Kareiva, P. 1983. Local movement in herbivorous insects: applying a passive diffusion model to mark-recapture field experiments. Oecologia **57**:322–324.

Kenyon, K. W. 1969. The sea otter in the eastern pacific ocean. U.A. Fish. Wildl. Serv. No. AM. Fauna **68**:1–352.

Kot, M. 2003. Do invading organisms do the wave? Canadian Applied Mathematics Quarterly **10**:139–170.

Kot, M., M. A. Lewis, and P. van den Driessche. 1996. Dispersal data and the spread of invading organisms. Ecology **77**:2027–2042.

Krkošek, M., J. Lauzon-Guay, and M. A. Lewis. 2007. Relating dispersal and range expansion of california sea otters. Theoretical Population Biology **71**:401–407.

Kvitek, R. G., J. S. Oliver, A. R. DeGange, and B. S. Anderson. 1992. Changes in alaskan soft-bottom prey communities along a gradient in sea otter predation. Ecology **73**:413–428.

Laidre, K. L., R. J. Jameson, and D. P. DeMaster. 2001. An estimation of carrying capacity for sea otters along the california coast. Marine Mammal Science **17**:294:309.

Laidre, K. L., R. J. Jameson, S. J. Jeffries, S. J. Hobbs, C. E. Bowlby, and G. R. VanBlaricom. 2002. Estimates of carrying capacity for sea otters in washington state. Wildlife Society Bulletin **30**:1172–1181.

Lubina, J. A. and S. A. Levin. 1988. The spread of a reinvading species - range expansion in the california sea otter. American Naturalist **131**:526–543.

Mack, R. N., D. Simberloff, W. M. Lonsdale, H. Evans, M. Clout, and F. A. Bazzaz. 2000. Biotic invasions: Causes, epidemiology, global consequences, and control. Ecological Applications **10**:689–710.

Monnett, C. and L. M. Rotterman. 2000. Survival rates of sea otter pups in alaska and california. Marine Mammal Science **16**:794–810.

Monson, D. H. and A. R. DeGrange. 1995. Reproduction, preweaning survival, and survival of adult sea otters at kodiak island, alaska. Can. J. Zool. **73**:1161–1169.

Murray, J. D. 2002. Mathematical Biology. Springer-Verlag.

Ostfeld, R. S. 1982. Foraging strategies and prey switching in the california sea otter. Oecologia **53**:170–178.

Press, W., S. Teukolsky, W. Vetterling, and B. Flannery. 2002. Numerical Recipes in C++: The Art of Scientific Computing. 2 edition. Cambridge University Press, Cambridge.

Riedman, M. L., J. A. Estes, M. M. Staedler, A. A. Giles, and D. R. Carlson. 1994. Breeding patterns and reproductive success of california sea otters. Journal of Wildlife Management **58**:391–399.

Shigesada, N. and K. Kawasaki. 1997. Biological invasions : theory and practice. 1st edition. Oxford series in ecology and evolution, Oxford University Press, Oxford ; New York.

Skellam, J. G. 1951. Random dispersal in theoretical populations. Biometrika **38**:196–218.

Taper, M. L., 2004. Model identification from many candidates. Pages 488–524 *in* M. L. Taper and S. R. Lele, editors. The nature of scientific evidence: statistical, philosophical, and empirical considerations. University of Chicago Press, Chicago.

Taper, M. L. and P. J. P. Gogan. 2002. The northern yellowstone elk: density dependence and climatic conditions. Journal of Wildlife Management **66**:106–122.

Wendell, F. 1994. Relationship between sea otter range expansion and red abalone abundance and size distribution in central california. California Fish and Game **80**:45–56.

Wendell, F. E., R. A. Hardy, J. A. Ames, and R. T. Burge. 1986. Temporal and spatial patterns in sea otter, *Enhydra lutris* range expansion and in the loss of pismo clam fisheries. California Fish and Game **72**:197–212.

Wikle, C. 2003. Hierarchical bayesian models for predicting the spread of ecological processes. Ecology **84**:1382–1394.

This 2-column preprint was prepared with the AAS LaTeX macros v5.2.